Int. J. Multiphase Flow Vol. 8, No. 3, pp. 217-226, 1982
Printed in Great Britain.

0301-9322/82/0301217-10$03.00/0
Pergamon/Elsevier

SEPARATED TWO-PHASE FLOW IN A NOZZLE

W. R. MARTINDALE
Dept. of Mechanical Engineering, Montana State University, Bozeman, MT 59717, U.S.A.

and

R. V. SMITH
Dept. of Mechanical Engineering, Wichita State University, Wichita, KS 67208, U.S.A.

(*Received* 12 *March* 1979; *in revised form* 24 *August*, 1981)

Abstract—This work was performed to extend and further test the method of handling separated two-phase flow by studying each phase separately and, particularly, by placing emphasis on the study of the gas phase with interface transport expressions showing the influence of the liquid phase on it. A one-dimensional flow model for accelerating flows was used in conjunction with experimental data to obtain the pressure distribution and velocity distribution in a converging nozzle for several values of flow quality and nozzle inlet stagnation pressure. The results tend to support the use of the model (which includes the assumption that the gas is in critical flow when the two-phase mixture is in critical flow) and give some insight regarding the nature of the liquid distribution near the nozzle throat.

INTRODUCTION

The purpose of this work was to extend and further test the method of analyzing separated two-phase flow by studying each phase separately, and particularly, by placing emphasis on the gas phase with interface transport expressions showing the influence of the liquid phase on it. The analyses of two-phase flow in the separated region tend to divide themselves between studies of the separated phases and studies in which effective mixture properties are used. This study falls in the first category and becomes an extension of previous separated-phase work. The analytical model has some new support from recently reported sonic velocity data and utilizes new experimental data, detailed data on the flow pattern, specifically on the liquid distribution on the wall and the droplet size and size distribution. It also made use of new data on the momentum transport at the liquid-gas interface. The experimental fluids were air and water.

Previous works using the separated-flow model were reported by Warner & Netzer (1963), Wallis & Sullivan (1972), Carofano & McManus (1969), and Smith (1968). These works all use separate equations to describe the behavior of each phase and the results tend to show the primary influence of the gas flow. More recent sonic velocity data to support the separate-phase concept have been reported by Martindale & Smith (1980a). This study shows the velocity of the leading edge of the pressure disturbance in a flowing two-phase mixture is essentially independent of the liquid flow rate from all-gas flow until the liquid flow rates is sufficient to change the flow region from separated flow. The interface momentum transport data were obtained from the same system and will be reported in Martindale & Smith (1980b). There have been substantial contributions to the droplet size data in recent years. The data for this study is based upon that obtained from the same system and is reported in Lindsted (1977).

The procedure, then, was to carry out parallel experimental and analytical studies utilizing these new data and concepts to compare analytically predicted experimental pressure drop and flow rate in a nozzle for both subcritical and critical flows.

ANALYSIS

The analytical model is shown schematically in figure 1. The basic system was to write equations for energy and momentum for the gas flow, and for the liquid flow at the wall and for the liquid flow entrained as droplets. Then the interface transport equations show the momen-

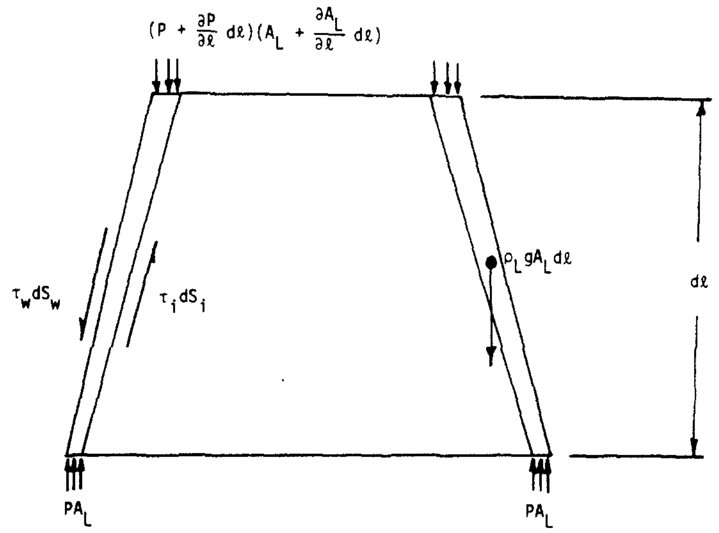

Figure 1. Liquid film force balance.

tum and energy transport between the phases. The final equations to be programmed for a numerical solution are as follows.

For the pressure drop

$$\frac{\mathrm{d}P}{\mathrm{d}l}=\frac{-C_{D_i}\dfrac{\rho_G}{2}(V_G-V_L)^2\pi D_G-C_{D_d}\dfrac{\rho_G}{2}(V_G-V_d)^2A_d-\dot m_G\dfrac{\mathrm{d}V_G}{\mathrm{d}l}}{A_G}. \qquad [1]$$

where P is the pressure, l is the axial length along the flow duct, C_{D_i} is the coefficient of gas-liquid film interface drag, ρ_G is the gas density, V_G is the gas velocity, V_L is the liquid velocity, D_G is the diameter of the gas flow area, C_{D_d} is the coefficient of droplet drag, A_d is the area of the droplet, $\dot m_G$ is the mass rate of flow of the gas, and A_G is the area of the gas core.

For the gas velocity

$$\frac{\mathrm{d}V_G}{\mathrm{d}l}=-\dot m_G\left(\frac{1}{\rho_G A_G^2}\frac{\mathrm{d}A_G}{\mathrm{d}l}+\frac{1}{\rho_G^2A_G}\frac{\mathrm{d}\rho_G}{\mathrm{d}l}\right). \qquad [2]$$

For the liquid-film velocity

$$\frac{\mathrm{d}V_L}{\mathrm{d}l}=\frac{C_{D_i}\dfrac{\rho_G}{2}(V_G-V_L)^2\pi D_G-C_{D_w}\dfrac{\rho_L}{2}V_L^2\pi D_T-\rho_LA_L-A_L\dfrac{\mathrm{d}P}{\mathrm{d}l}}{\dot m_L}. \qquad [3]$$

where C_{D_w} is the coefficient of duct wall drag, ρ_L is the density of the liquid, D_T is the total duct diameter, $\dot m_L$ is the mass rate of flow of the liquid. This is for the liquid film velocity which is assumed to be substantially slower than the droplet velocity because the momentum transport to the droplet from the gas is much more effective than the momentum transport to the liquid wall film. The droplet velocity is shown in [8].

For the temperature of the gas

$$\frac{\mathrm{d}T_G}{\mathrm{d}l}=\left[\frac{h_LS_L\left(\dfrac{\mathrm{d}T_L}{\mathrm{d}l}-\dfrac{\mathrm{d}T_G}{\mathrm{d}l}\right)+h_L\dfrac{\mathrm{d}S_L}{\mathrm{d}l}(T_L-T_G)}{C_{P_G}\dot m_G}+\frac{h_dS_d\left(\dfrac{\mathrm{d}T_L}{\mathrm{d}l}-\dfrac{\mathrm{d}T_G}{\mathrm{d}l}\right)}{C_{P_G}\dot m_G}\right]-\frac{V_G}{C_{P_G}}\frac{\mathrm{d}V_G}{\mathrm{d}l}. \qquad [4]$$

where T_g is the temperature of the gas, h_L is the convective heat transfer coefficient at the film-gas interface, S_L is the surface area of the liquid film-gas interface, h_d is the convective heat transfer coefficient for the droplet, S_d is the surface area of the droplet, d is the droplet diameter, C_{P_G} is the specific heat at constant pressure for the gas.

For the temperature of the liquid

$$\frac{\mathrm{d}T_L}{\mathrm{d}l}=\frac{-(h_LS_L+nh_dS_d)\left(\frac{\mathrm{d}T_L}{\mathrm{d}t}-\frac{\mathrm{d}T_G}{\mathrm{d}l}\right)-h_L\frac{\mathrm{d}S_L}{\mathrm{d}l}(T_L-T_G)-h_d\frac{\mathrm{d}S_d}{\mathrm{d}l}(T_d-T_g)}{C_{PL}\dot{m}_{L_d}}-\frac{V_L}{C_{P_L}}\frac{\mathrm{d}V_L}{\mathrm{d}l} \qquad [5]$$

where n is the number of droplets in a differential volume element, m_{L_d} is the combined mass rates of the liquid and droplet flows, and $\mathrm{d}S_d/\mathrm{d}l$ is assumed equal to zero. In this equation, it is assumed that the film liquid and the liquid as droplets have the same temperature. This is because there is a constant mass interchange between the entrained droplets redepositing on the liquid film, and the tearing away of droplets from the liquid film and subsequent entrainment. While this assumption may not be entirely accurate near the throat where the gas temperature and that the droplet temperature may be changing rather rapidly, even relatively large deviations at that point will not substantially change the results.

For the density of the gas, assuming ideal gas behavior

$$\frac{\mathrm{d}\rho_G}{\mathrm{d}l}=\frac{1}{RT_G}\frac{\mathrm{d}p}{\mathrm{d}l}-\frac{p}{RT_G^2}\frac{\mathrm{d}T_G}{\mathrm{d}l}. \qquad [6]$$

where R is the gas constant.

For the effective area for the gas flow

$$\frac{\mathrm{d}A_G}{\mathrm{d}l}=\frac{\mathrm{d}A_T}{\mathrm{d}l}+\frac{\dot{m}_L}{\rho_L V_L^2}\frac{\mathrm{d}V_L}{\mathrm{d}l}. \qquad [7]$$

And for the velocity of the droplets

$$\frac{\mathrm{d}V_d}{\mathrm{d}t}=\frac{C_{D_d}\frac{\rho_G}{2}(V_G-V_d)^2A_d}{m_dV_d}. \qquad [8]$$

In the preceding expressions, A_G is the total area less the area occupied by the liquid. Additionally, there are voids behind the droplets and in the wave troughs on the liquid film which represent areas filled by gas moving at a low velocity relative to the remainder of the gas in the core. A further correction for these slow-moving gas areas is shown in [11]. This expression will give a substantially different liquid velocity for the droplets than that expressed for the film in [3].

The energy transport coefficients are from standard expressions from the literature. The film coefficient for the liquid-film and gas interface is a correlation of the form proposed by Dittus–Boelter (1930). The heat transfer coefficient between the droplet and the gas is from Ranz-Marshall (1952). The drag coefficients for the droplets were from Rabin *et al.* (1960). The drag coefficient between the liquid-film at the wall and the wall was a standard form with the coefficient evaluated at 0.0015. This value was one chosen from a laminar film analysis and partially from the results of this and the interface drag coefficient which is discussed next.

The interface drag coefficient for the liquid film was determined by a separate study reported by Martindale & Smith (1981). The results of this analysis showed the interface coefficient to be a relatively strong function of the quality, or of the liquid film thickness, and the gas velocity. As a result of that study the variations in the drag coefficient were determined

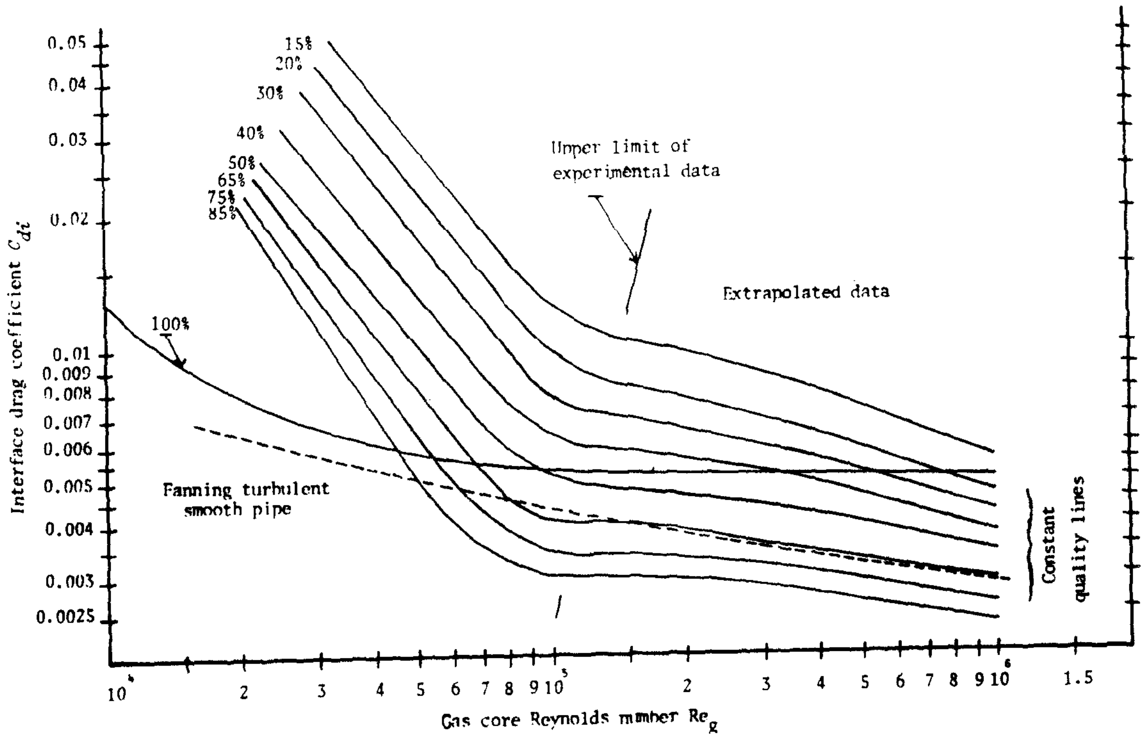

Figure 2. Constant area flow model prediction of interface drag coefficient.

and these are shown in figure 2. Second order spline-fit equations were used to relate the interface drag coefficient values as a function of the gas core Reynolds number for use in the numerical solution.

The effective droplet size and distribution was developed from direct experimental observations in an open pipe at the entrance to the test nozzle. The droplet size was directly related to the photographic data obtained for any equivalent condition to the entrance as reported by Lindsted (1977). For the change in droplet size during the flow through the nozzle the break-up criteria proposed by Rabin *et al.* (1960) was used.

$$\frac{\mathrm{We}}{(\mathrm{Re})^{0.5}} = \frac{\rho_L (V_G - V_d)^2 \dfrac{D_d}{\sigma}}{\left[(V_G - V_d)\dfrac{D_d}{\nu_G}\right]^{0.5}} > 1. \qquad [9]$$

where We is the Weber number, Re is the Reynolds number, σ is the surface tension, ν_G is the dynamic viscosity of the gas. Thus the droplet break up and new effective diameter was determined using the above criteria.

In order to account for regions which partially block the gas flow, such as the trough area of waves occurring on the liquid interface and the areas behind entrained droplets, a blockage factor was employed. This blockage factor was employed in the following form:

$$A_g' = Ag(1 + BF) - A_T(BF) \qquad [10]$$

where a modified gas core flow area is calculated. The modified area term is used as the gas core area in [1] and [2] only. The original use of this blockage factor was an empirical derivation of critical mass flow rates by Smith (1972). This study used experimental evaluations of a blockage factor obtained by Lindsted (1977) which was defined by

$$\text{B.F.} = \frac{A_T - A_\delta - A_d - A_w}{A_T - A_\delta} \quad [11]$$

where A_δ is the area of the liquid film, A_T is the total area of the duct, A_w is the wave height above the mean film thickness. These areas used to determine the blockage factor were obtained from analysis of a very large number of droplet and wave photographs in the same flow loop, Lindsted (1977). Lindsted considered the influence of waves and wakes with measured values for the waves and the assumption that the wake behind the droplet was conical and approximately 5 times the diameter of the droplet.

The liquid quantity entrained in the gas core was determined partially empirically and partially from experimental data. The average number of droplets in any given plane was taken from the Lindsted (1977) data, however the distance between the planes was determined from the entrainment data of Wallis (1962). During the numerical integration of flows which were verified to be critical flows from the experimental data, the nozzle inlet entrainment fraction was varied until critical flow was predicted at the nozzle exit. This variation is shown in figure 3. The model consistently overpredicted the exit pressure when the entrainment fraction was less than the value shown in figure 3.

Data taken in a constant area duct for sonic velocity behavior as a function of flow quality indicate that the water exerts very little influence on pressure pulse propagation velocity in the gas phase, (Martindale & Smith 1980a). This behavior was found to be consistent down to a quality of 10%. Below 10% quality the flow pattern was noticeably changed to a mixing flow as opposed to the separated phase, annular flows existing for higher qualities. Below 10% quality the sonic velocity was significantly reduced indicating that the continuous gas phase is being blocked as during a flow pattern transition to churning flow. A full discussion of this sonic velocity data can be found in Smith *et al.* (1975).

For the case of critical flows in the nozzle, the gas phase governed choking of the flow. As the quality decreased the amount of entrainment was increased as figure 3. This is indicative of the flow pattern development occurring when a transition from separated-annular to churning flow is occurring. Figure 3 seems to show this transition near 10% quality just as did the sonic velocity behavior.

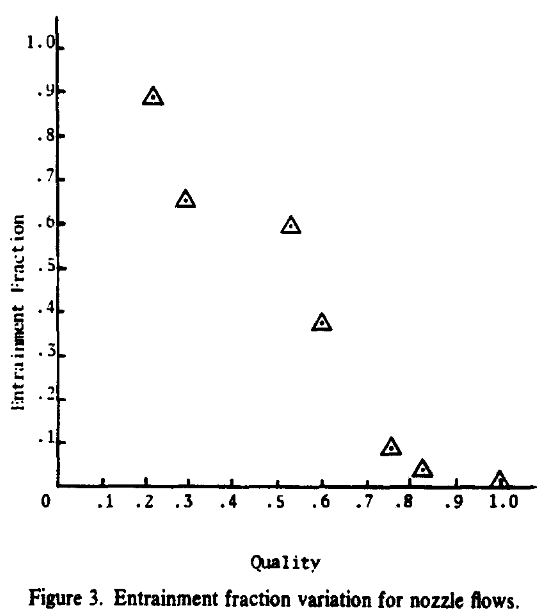

Figure 3. Entrainment fraction variation for nozzle flows.

EXPERIMENTAL

The experimental system for nozzle flows is shown in figure 4. The nozzle itself is shown in figure 5. This nozzle was designed according to ASME specifications and exhausted into an abrupt expansion at the exit plane from a diameter of 1.27 cm to 3.51 cm. This nozzle was instrumented with 16 pressure taps, 1.59 mm i.d. located 2.54 mm apart and regularly spaced

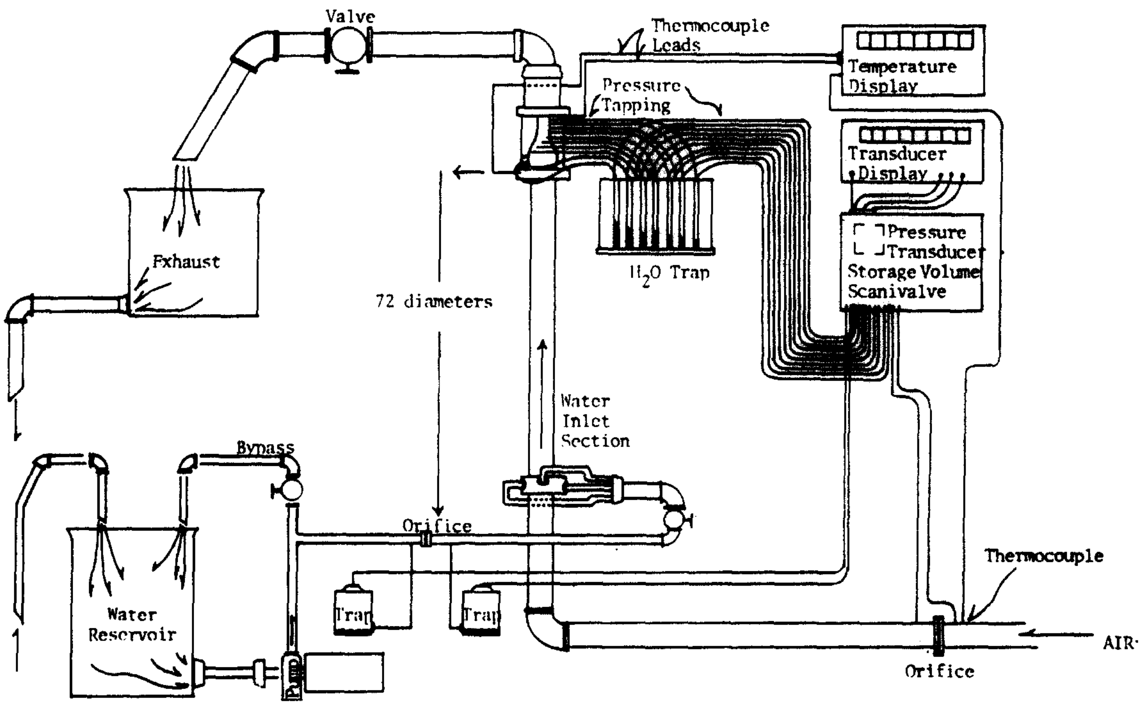

Figure 4. Experimental system schematic for nozzle flow measurements.

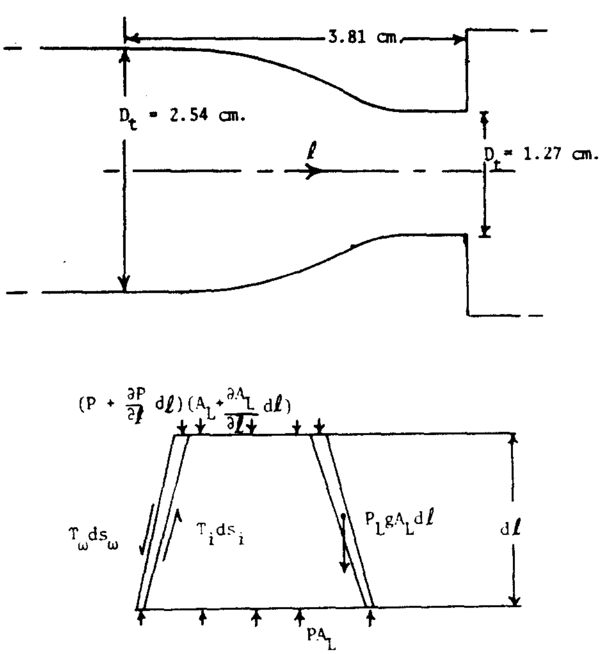

Figure 5. Nozzle flow duct geometry.

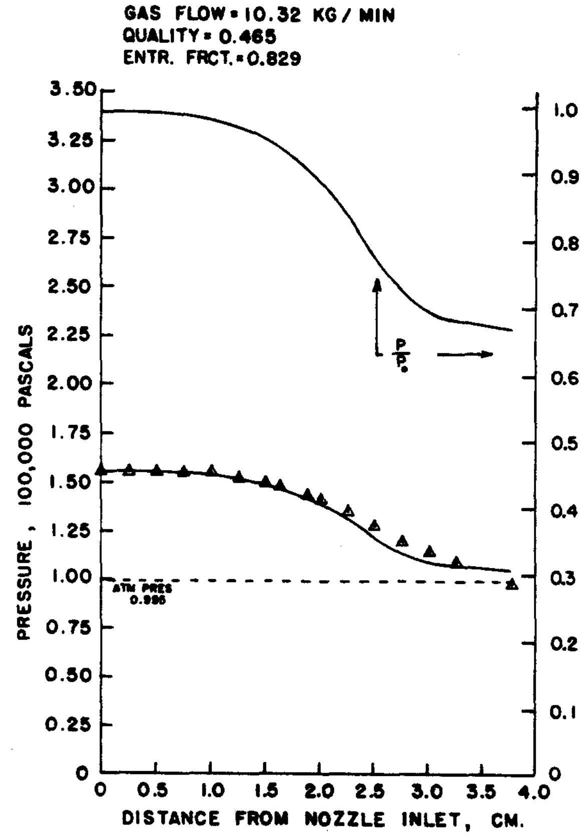

Figure 6. Experimental and predicted pressure profile through nozzle.

along the nozzle length. The last pressure tap was located just inside the nozzle exit plane. Air flow rates were determined by metering through a previously calibrated orifice. The water flow rate was determined from a time period weighing at the exhaust of the system after the air had separated. Typical subsonic flow results are shown in figure 6 and typical critical flow results are found in figure 7. The experimental and theoretical comparisons are shown on the pressure curve and the calculations of the pressure curve and the calculations of the pressure over the stagnation pressure is shown in the upper curve on the figure. The critical pressure ratios were near the value for critical flows of air alone. Sonic velocity data indicated this could be expected. Additionally, the temperatures and gas velocity and area flow ratios were calculated and are shown in figures 8 and 9. For complete results see Martindale (1977).

DISCUSSION

The system for comparison of the analytical and experimental data, which would show the reliability of critical flow predictions of the analytical equations, is as follows. The equations must first predict the critical flow rate. They did this, requiring only minor adjustments in the percentage of entrained liquid flow (figure 3). Once this empirical adjustment was made, those values were used for all cases and typical results are reported in this paper. The critical flow prediction test involved both the critical flow rate and the critical pressure. The experimental critical pressure is always difficult to determine and in this case should be considered a compromise between the measurement at the exit plane, which is known to be somewhat inaccurate, and the extrapolation of the experimental pressure profile. The critical pressure prediction from the analytical equations seems adequate, especially considering the uncertainties of the experimental determination.

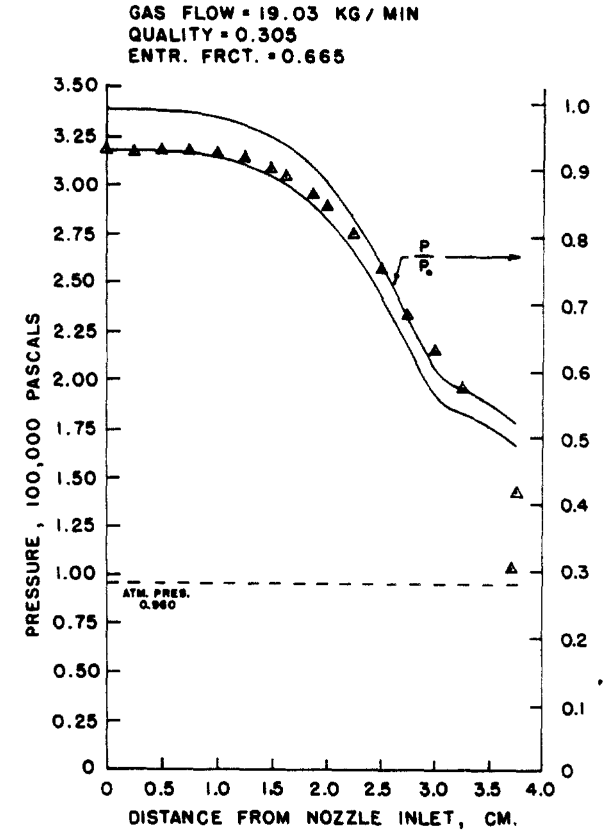

Figure 7. Experimental and predicted pressure profile through nozzle.

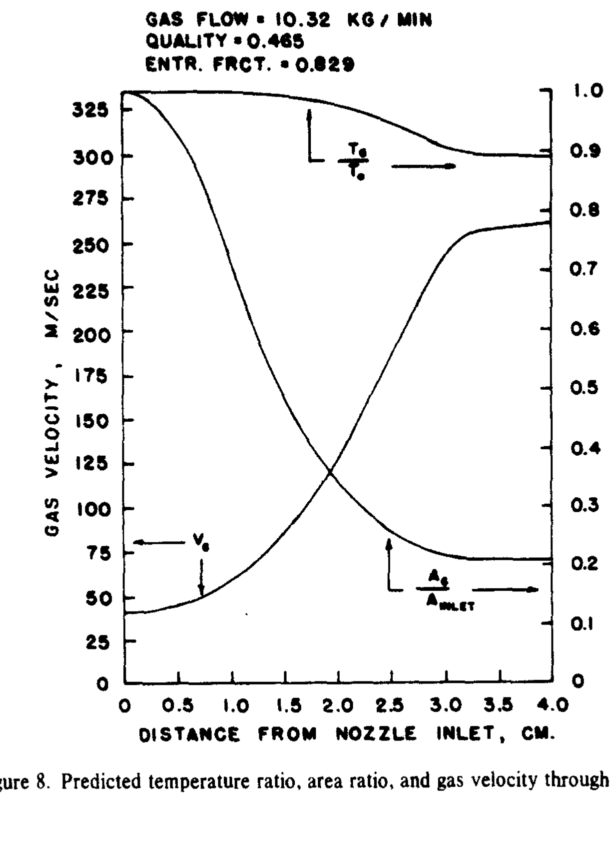

Figure 8. Predicted temperature ratio, area ratio, and gas velocity through nozzle.

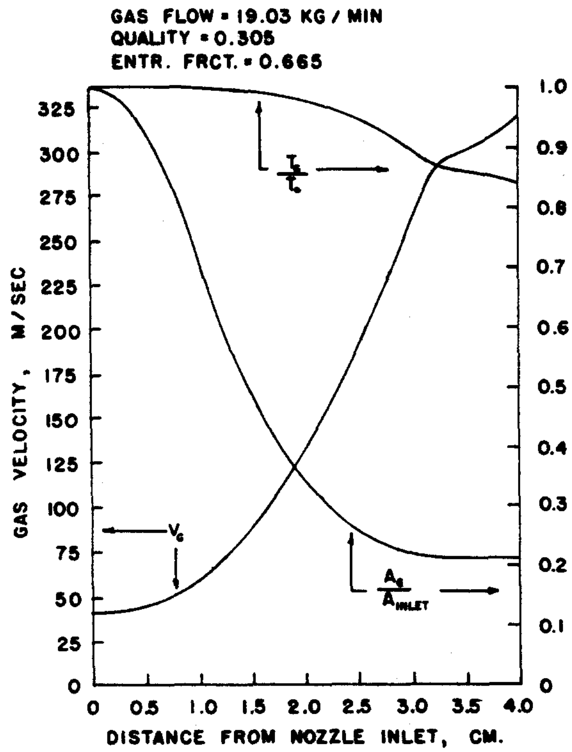

Figure 9. Predicted temperature ratio, area ratio, and gas velocity through nozzle.

In addition to the comparisons of the flow rate and critical pressure, the equations were tested to simulate the pressure profile. For this region of separated flow where there is a large volume ratio of gas flow to liquid flow, it is known that a number of models are reasonably successful in predicting both the critical flow rate and pressure. Therefore, further substantiation may be obtained by comparing the pressure profiles. Other analytical models will produce a critical pressure of approximately the values shown here. However, they often do not produce an accurate upstream pressure profile.

The agreement between the analytical and experimental work indicates the method to be accurate to the degree which might reasonably be expected. The model, although still imperfect and dependent upon some empiricism, is more soundly based than those previously reported, particularly with respect to the description of the liquid-gas flow pattern and with respect to the gas-liquid film interface.

CONCLUSIONS

(1) The concept of using a separated flow model, with separate equations for each phase, is further substantiated by these results. In this model, the gas flow is studied using an effective gas flow area with interface transport expressions to account for the presence of the liquid. This gas-flow area was based on the experimental measurements of liquid films and droplets.

Additionally, for the separated flow region, the gas is assumed to be in critical flow when the two-phase mixture is in critical flow. This assumption is supported by the analytical and experimental agreement for the critical pressure ratio and critical flow rate and nozzle pressure profile. These results are in agreement with previous works using a separated flow model.

(2) The range of validity of the separated flow model was not rigorously investigated but the pressure-drop data, the entrainment variation and the sonic velocity data all seem to point that, for these pressures, the model is valid down to the range of 10–20% quality where the flow regime changes. The transition between separated flow and mixed flow is further established in

this quality range by sonic velocity measurements showing the change in pressure pulse propagation speeds.

Acknowledgements—The authors would like to acknowledge the support from the National Science Foundation Grant GK38425 which was active in the first portion of this study. The authors would also like to acknowledge the assistance of Dr. R. D. Lindsted whose counsel and data were extremely valuable to the results shown herein.

REFERENCES

CAROFANO, G. C. & MCMANUS, H. N., Jr. 1969 An analytical and experimental study of the flow of air–water and steam–water mixtures in a converging–diverging nozzle. *Progress in Heat and Mass Transfer*, Vol. 2. Pergamon Press, Oxford.

DITTUS, F. W. & BOELTER, L. M. 1930 *Heat Transfer in Automobile Radiators of the Tabular Type*, Vol. 2. University of California Publ: Engr.

LINSTED, R. D. 1977 A photographic technique to obtain droplet and flow pattern data in two-phase flow for use in modeling. Ph.D. Thesis, University of Oklahoma. Also with Smith R. V. 1979 *Proc. of 2nd Multi-Phase and Heat Transfer Symp.* University of Miami.

MARTINDALE, W. R. 1977 Two-phase air–water upward annular flow in a converging nozzle. Ph.D. Thesis, Wichita State University, Wichita, Kansas.

MARTINDALE, W. R. & SMITH, R. V. 1981 Two-phase, two-component interface drag coefficients in separated phase flow, *Int. J. Multiphase Flow.* **7**, 211–219.

MARTINDALE, W. R. & SMITH, R. V. 1980a Sonic velocity and pressure drop in separated two-phase flow. *Trans. ASME J. Fluids Engng* **102**, 112–114.

RABIN, E., SCHALLENMULLER, A. R. & LOWHEAD, R. B. 1960 Displacement and shattering of propellant droplets. *Final Summary Report AFOSR TR* 60–75. Rocketdyne, a Division of North American Aviation, Inc.

RANTZ, E. W. & MARSHALL, W. R., Jr. 1952 Forced convection heat transfer from a single sphere. *Chem. Engng Prog.* **48**, 000–000.

SMITH, R. V. 1968 Two-phase, two-component, critical flow in a Venturi. D. Phil. Thesis, University of Oxford, England, Also 1972 *J. Basic Engng* **94**, (147–155) and with Cousins, L. B., and Hewitt, G. F. 1968 *UKAEA Report AERE*-R5736.

SMITH, R. V., MARTINDALE, W. R. & LINDSTED. R. D. 1975 Two-phase sonic velocity measurements for separated flow. *ASME Paper #*75 WA/HT-34.

Wallis, G. B. 1962 Entrainment for air–water downflow. *General Electric G. Report* 62*GL*127, Schenectady, New York.

Wallis, G. B. & Sullivan, D. A. 1972, Two-phase air–water nozzle flow. *J. Basic Engng* **94**, 788–794.

WARNER, C. F. & NETZER, D. W. 1963 An investigation of the flow characteristics of two-phase flow in converging–diverging nozzles. *ASME Paper No.* 63-*WA*-192.